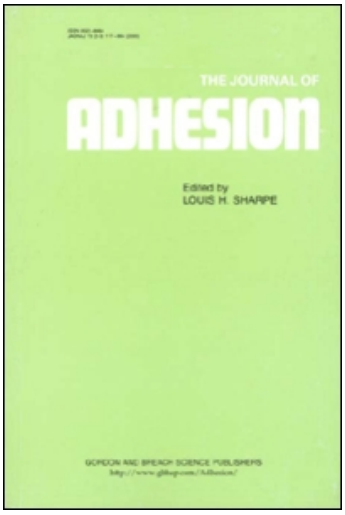

The Journal of Adhesion

Publication details, including instructions for authors and subscription information:
http://www.informaworld.com/smpp/title~content=t713453635

Adhesion Science and Surface Analysis. Typical Examples

M. Romand[a]; F. Gaillard[a]; M. Charbonnier[a]; N. S. Prakash[a]; L. Deshayes[a]; I. Linossier[a]
[a] Laboratoire de Chimie Appliquée et Génie Chimique (CNRS, ERS 069), Université Claude Bernard, Villeurbanne Cedex, France

To cite this Article Romand, M. , Gaillard, F. , Charbonnier, M. , Prakash, N. S. , Deshayes, L. and Linossier, I.(1995) 'Adhesion Science and Surface Analysis. Typical Examples', The Journal of Adhesion, 55: 1, 1 — 16
To link to this Article: DOI: 10.1080/00218469509342403
URL: http://dx.doi.org/10.1080/00218469509342403

J. Adhesion, 1995, Vol. 55, pp. 1–16
Reprints available directly from the publisher
Photocopying permitted by license only

Adhesion Science and Surface Analysis. Typical Examples

M. ROMAND, F. GAILLARD, M. CHARBONNIER, N. S. PRAKASH, L. DESHAYES and I. LINOSSIER

Laboratoire de Chimie Appliquée et Génie Chimique (CNRS, ERS 069), Université Claude Bernard-LYON 1, 43 boulevard du 11 November 1918, 69622 VILLEURBANNE CEDEX, FRANCE

(Received August 4, 1994; in final form December 12, 1994)

A number of surface modification methods using mechanical, chemical, electrochemical or physical processes have commonly been employed to treat adherend surfaces and improve adhesion in various bi- or multi-layered systems which play a key role in many advanced technologies. Results reported in this review paper deal more particularly with components of polymer-metal systems and provide typical examples of surface analysis obtained by x-ray photoelectron spectrometry (XPS), ion scattering spectrometry (ISS), low-energy electron induced x-ray spectrometry (LEEIXS), optically stimulated electron emission (OSEE) and Fourier transform infra-red spectrometry (FTIR). These examples concern, on the one hand, metallic adherends (aluminum, stainless steel, zinc-coated steel, gold) the surfaces of which were modified by cleaning, etching, oxidation, conversion or chemical grafting and, on the other hand, bonded joints (polyester-steel and epoxy-aluminum systems) which were delaminated using a peel test and a three-point flexure test, respectively.

KEY WORDS Surface analysis; XPS; ISS; FTIR; low energy electron induced spectrometry (LEEIXS); optically stimulated electron emission (OSEE); surface treatment; surface cleaning; surface etching; surface oxidation or conversion; surface grafting; adhesion science; metallic substrates; mechanical measurement; three-point flexure test; peel test; bonded joints.

INTRODUCTION

In the past few years, adhesion phenomena, particularly in polymer-metal or metal-polymer systems, have been shown to play a key role in many important areas of modern science and technology. To mention only a few examples, areas which have received much attention are those concerning (i) adhesive bonding and corrosion protection of metallic substrates by thin or thick organic coatings such as paints, varnishes, etc., (ii) metallization of plastics and (iii) adhesion in filler or fiber-reinforced composites and in blends (polymer mixtures). In this context, it should be pointed out that the significant progress made in the understanding of the various chemical, physical and mechanical factors which lead to adhesion or to adhesion loss are the result, to a large extent, of the availability and development of suitable analytical

* One of a Collection of papers honoring James P. Wightman, who received the 13th Adhesive and Sealant Council Award at the ASC's 1993 Fall Convention in St. Louis, Missouri, USA, in October 1993.

techniques. As may clearly be apparent from the recent and less-recent literature[1-10] these techniques are capable of probing adherend surfaces at each step of their preparation, as well as of investigating the interfacial interactions occuring between adherend and adherate when the two materials are brought together and/or when the adhering systems have suffered degradation and failure. The present paper illustrates some examples of works which are commonly performed in the authors' laboratory. More particularly, the relevant applications relate to the characterization both of surfaces and thin films developed to improve performances of bonded joints, and of mechanically-failed specimens.

EXPERIMENTAL

Results provided in this paper were obtained by x-ray photoelectron spectrometry (XPS), ion scattering spectrometry (ISS), low-energy electron induced x-ray spectrometry (LEEIXS), optically stimulated electron emission (OSEE) and Fourier transform infra-red spectrometry (FTIR).

XPS measurements were carried out on a Riber SIA 200 instrument using a non-monochromatized X-ray source (Mg K_α at 1253.6 eV or Al K_α at 1486.6 eV) and a Mac 2 energy analyzer. The vacuum in the analytical chamber was better than 1.10^{-9} Torr, and the electron take-off angle was 65° with respect to the sample surface, unless otherwise specified in the text. Analyses were carried out on 1 × 1.2 cm rectangular samples. Survey and high resolution spectra were taken using resolution of 2.3 and 0.9 eV, respectively. All the observed photoelectron peaks were corrected for charging effects by referencing to the C1s peak relative to hydrocarbon species at 284.6 eV. ISS experiments were also performed using the Riber SIA 200 system, the Mac 2 analyzer being capable of detecting ions instead of electrons when its entry polarity is inverted. Analyses were carried out with Ne^+ ions (2 keV, 500 nA) focused on a spot 0.5 mm in diameter. Operating vacuum in the analytical chamber was about 10^{-7} Torr.

LEEIXS measurements were carried out on a wavelength-dispersive X-ray spectrometer using an electronically-stabilized gas discharge tube which operates as an electron source under the primary vacuum (1–15 Pa range) of the spectrometer. A schematic representation of the experimental set-up is given in Figure 1. Typical operating conditions of the electron source were in the 1–5 kV range with a current between 0.1 and 0.2 mA, the diameter of the electron beam at the sample surface being less than 1 cm. Soft and ultra-soft X-rays (wavelengths in the 0.3–20 nm range) emitted in such conditions, and particularly K radiations from light elements, were dispersed by flat analyzing devices and detected by a flow proportional counter. Details about this technique are given in the literature.[11-13] It need only be recalled that this tool is capable of probing the surfaces and near-surfaces of materials typically up to about 100 nm, the corresponding depth depending, among other parameters, on the incident electron beam energy and the nature of the sample. In addition, it should be highlighted that LEEIXS can be used to probe the surfaces of non-conducting samples. Indeed, the charging effects commonly encountered in most surface analysis techniques operating in high and ultra-high vacuum conditions are not present with the source-type here considered. Although LEEIXS has been used in the present work to analyze ultra-thin

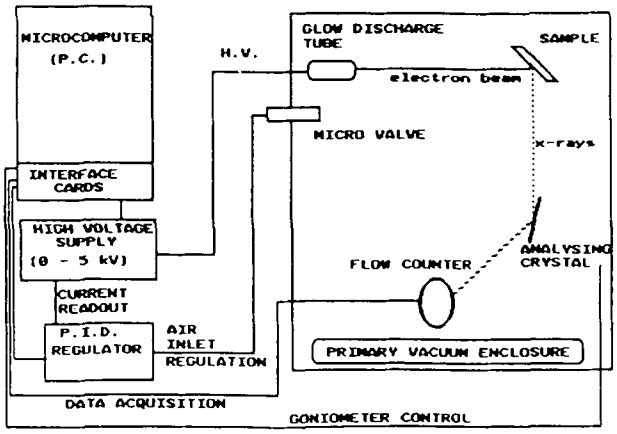

FIGURE 1 Schematic diagram of the LEEIXS Spectrometer.

films which would have been probed by XPS, let us recall that this x-ray emission technique has been shown to provide specific information which is not obtainable by the usual surface analysis methods (XPS, AES, SIMS or ISS) and sometimes obtainable, although in a rather difficult way, by electron probe microanalysis (EPMA). In this context, LEEIXS has been shown, for instance, to be a well-suited tool for controlling and optimizing thin film deposition as well as surface treatment processes.[12,13]

OSEE measurements were perfomed on a Photo Acoustic Technology OP 1020 instrument. The principle of this technique[14] consists of irradiating, at atmospheric pressure, the surface to be analyzed using UV rays emitted by a mercury vapor lamp and by collecting the photoelectron current thus emitted *via* a positively-biased grid. The irradiated zone is about 1 cm in diameter but it may be decreased by using suitable masks. Current-to-time graphs may be plotted *via* a computer. The sample may also be moved along x-y directions under the beam.

The FTIR spectra were recorded on a Nicolet 710 spectrometer. Microspectrometry was performed with a Nic-Plan device, fitted to the 710 bench, and equipped with both conventional (40°, × 15) and grazing incidence (84°, × 32) obejectives. Such a device allows one to select visually and then to analyze by FTIR (in the reflection or transmission mode) areas ranging from 20 to 250 μm in diameter. Heating cell experiments were performed with the multimode device #2000 from Aabspec.[15] This cell enables FTIR analysis in the transmission and reflection modes with controlled sample temperature (up to about 500°C) and with controlled cell atmosphere.

Adhesion testing was carried out using a three-point flexure method according to the AFNOR T 30 010. A schematic representation of the test set-up and of the adherend/adhesive specimen geometry[16-18] are shown in Figure 2. It should be mentioned here that this test has already shown its potential, not only in evaluating the effects of various adherend treatments, but also in optimizing, for a given treatment, the experimental conditions to be chosen in order to promote better adhesion. Flat adherend sheets, about 1 mm in thickness, were prepared by die-cutting to provide identically-sized strips (50 × 10 mm) and were then subjected, prior to bonding, to

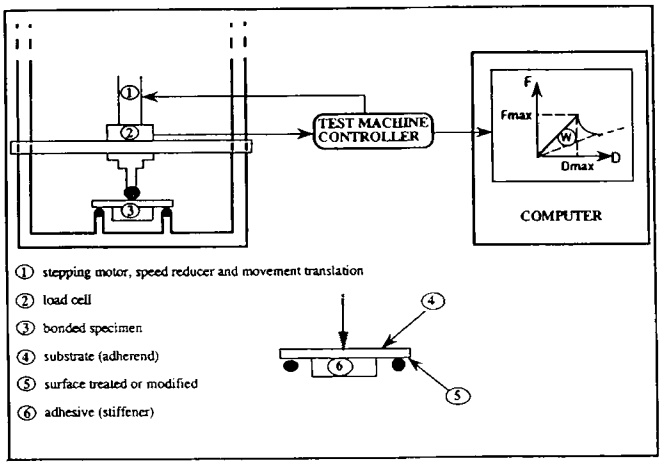

FIGURE 2 Schematic representation of the three-point flexture test.

different surface treatments. The adhesive employed (3525 B/A from 3M) in all cases was cured by heating the joint at 80°C for 2 hours. The bonded specimens were stored for 24 hours in a controlled atmosphere (20°C at 50% RH) and then tested. The computer-controlled testing machine (Flex 3 from Techmetal, France) maintains the cross-head displacement at a rate of 0.5 mm.min^{-1}, records the conventional load/displacement curve and helps to determine the parameters of interest. In this work, the practical adhesion of the systems investigated was determined by measuring either the ultimate load value or the energy associated with the failure initiation of the adhering system. Such values provide a relative indication of the bond strength at (and near) the substrate/film interface. It, therefore, allows one to compare the effects of various adherend treatments and of the characteristics of the film itself. In each case, a series of six specimens was studied in order to obtain statistical reproducibility. In each figure providing adhesion data, results for each series are represented by a rectangle whose height indicates the statistical error ($\pm \sigma$) and whose central point indicates the average value.

Some joint strength measurements were also obtained using a floating roller test (peel joints according to a modified ASTM test method D 3167–76).

Plasma treatments were performed in a Plasma Technology cylindrical reactor (RIE 80 model) which consists of two parallel electrodes (4 cm apart, 17 cm in diameter). This system is fed by an inductively-coupled power source operating up to 300 W at a radio-frequency of 13.56 MHz. Other parameters of interest are given for each application.

RESULTS AND DISCUSSION

Surface and Thin Film Characterization Before Bonding

Surface pretreatments of metallic materials are frequently carried out before bonding. As has now been well established by a number of researchers, pretreatments may be

simple or complex, depending on the nature of the substrate and the service requirements. To achieve strong initial bonds, as well as long term durability of bonded joints, pretreatments of adherends must generally remove surface contaminants and weak boundary layers, increase surface roughness and provide new and more stable surface layers (*e.g.* oxide, phosphate, etc). For this purpose, mechanical, chemical, electrochemical or physical processes may be used.[19-23] In the following, some examples concerning surface characterization of metallic substrates which were subjected to cleaning, oxidation or chemical conversion, and grafting are given.

Surface cleaning

As is well-known, pretreatments of metals or alloys often consist of two preliminary phases which involve degreasing to remove organic contaminants and chemical etching to deoxidize their surface. Figure 3 refers to OSEE experiments on aluminum samples: (a) as received, (b) degreased ultrasonically for 5 min in a chlorinated solvent (stabilized 1,1,1-trichloroethane) and (c) etched in an alkaline medium (NaOH, 150 $g.l^{-1}$, pH 11) at room temperature for 1 min. The OSEE signal intensity gives evidence of the whole effect of the two surface pretreatments. Organic contaminations and alumina constituting the natural oxide of the substrate being, in fact, less photo-emitting than metallic aluminum, the signal intensity increases on the one hand after degreasing and on the other hand after etching. These capabilities of OSEE may, therefore, be used to determine the optimal duration of degreasing and etching treatments of various substrates. However, it must clearly be stated here that removing or minimizing the pre-existing oxide layer may not provide an optimum surface treatment of a metallic adherend and that, therefore, an additional surface treatment has generally to be carried out before bonding. Furthermore, it must also be recalled that OSEE alone may not discriminate between the effects of different surface treatments, it being possible for an identical signal intensity to result from different surface

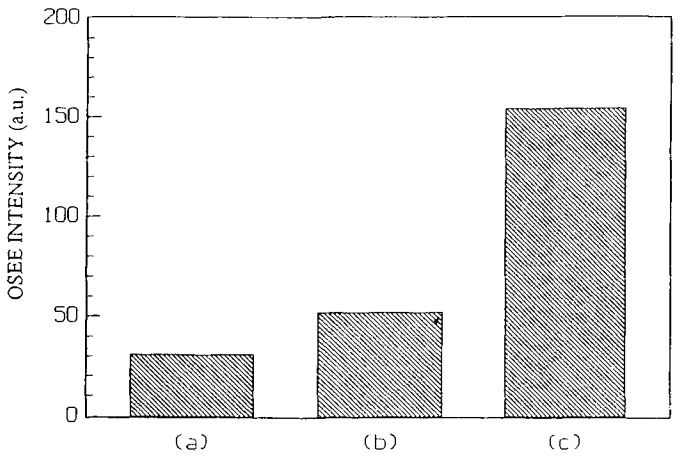

FIGURE 3 OSEE intensity from aluminum samples: (a) as-received, (b) degreased, and (c) chemically-etched.

chemical states. On the contrary, OSEE is quite capable of following the effects of a specific surface treatment, for instance as a function of treatment duration (see next paragraph).

Surface oxidation or conversion

Because metals or alloys are easily oxidized in air, it is often necessary to monitor the thickness of the oxide film which is spontaneously formed at their surface after an etching treatment. Figure 4 shows an example of this kind of study. It relates to the oxidation in air at room temperature of a freshly-etched copper sample in a concentrated HNO_3 bath. The OSEE technique allows one to determine a growth law for the oxide film. Such results are in agreement with data obtained by remission photometry[24] at a wavelength of 500 nm.

Similarly, Figure 5 represents the OSEE intensity variation from an AISI 430 stainless steel substrate subjected to an O_2 plasma treatment (power density =

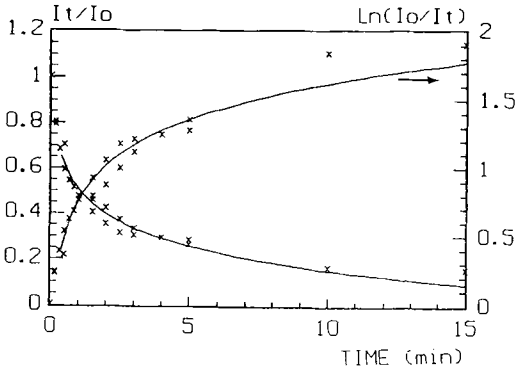

FIGURE 4 OSEE intensity evolution *vs.* time of a freshly etched copper sample.

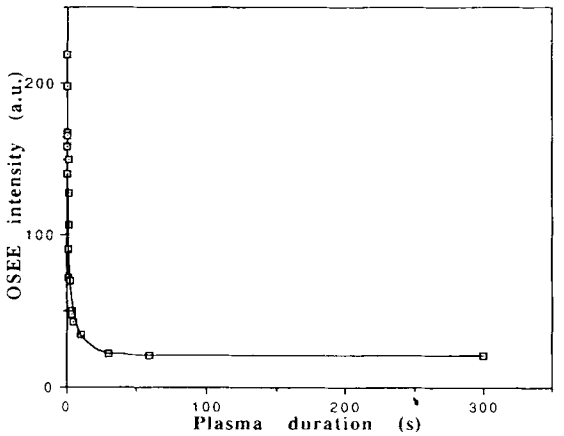

FIGURE 5 OSEE intensity evolution *vs.* time of an AISI 430 stainless steel sample subjected to an O_2 plasma.

$0.54\,W.cm^{-2}$; gas pressure = 100 mTorr; flow rate = 100 sccm) as a function of treatment duration. The corresponding signal intensity decreases rapidly until it reaches a minimum value at about 30 seconds and then remains more or less constant. This minimum level is associated with the formation of an oxidized layer, whose thickness is limited. Besides, the effects of the O_2 plasma at the first steps of the treament are shown in Figure 6. As can be seen, the OSEE signal intensity, in fact, begins to increase until 0.2 s and then decreases. The first part of the corresponding curve is obviously due to the removing of the hydrocarbon contamination layer by chemical (see next paragraph) and mechanical (ion etching) action. These results were supported by FTIR-IRRAS measurements.[25,26] In addition, the rate of the cleaning and oxidation phases was shown to be largely dependent on the plasma power density used. As can also be expected, the removing of the surface contaminants allows one to improve the initial bond strength of adhesive/stainless steel systems. Figure 7 illustrates the corresponding changes in adhesion properties as a function of plasma treatment duration. The highest bond strength was obtained here between about 0.2 and 1 s of treatment time, this duration range corresponding, presumably, to the complete removal of the contamination layer. However, it should be noted that OSEE alone is not a technique that can distinguish the two processes involved, viz. the cleaning and the oxidation, of any metallic surface and, therefore, of the stainless steel surface considered in this work.

It should now be recalled that etching (deoxidizing) alone of a metallic substrate is generally an inadequate surface treatment to achieve long-term service life of bonded structures, and that bond durability may be largely improved when adherend surfaces are prepared, prior to bonding, by using a variety of additional chemical, electrochemical or physical treatments. In this context, metals such as aluminum, titanium, stainless steel, etc., are commonly subjected to oxidation processes *via* suitable chemical etching, anodization or plasma procedures. Most of these processes were experimented within our laboratory and surface analysis was carried out to characterize their different steps. By way of example, plasma treatments using O_2 as the reactive gas were carried out on

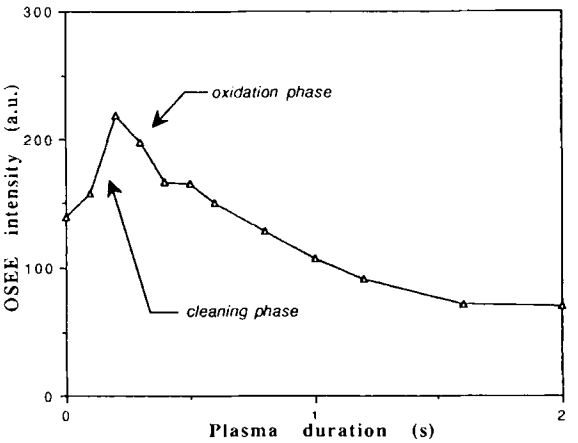

FIGURE 6 OSEE intensity evolution *vs.* time of an AISI 430 stainless steel sample subjected to an O_2 plasma (first steps of the treatment).

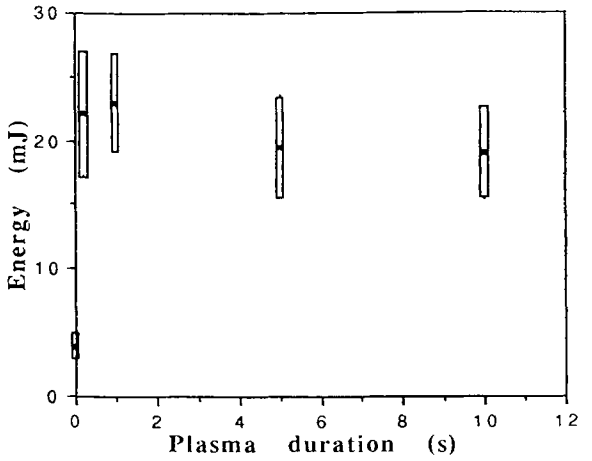

FIGURE 7 Effect of the O_2 plasma treatment of the substrate on the bond strength of epoxy/AISI 430 joints. (Three-point flexure test measurements)

an AISI 304 L stainless steel in order to obtain a better understanding of the effects of such treatments on the surface composition. Samples treated under a variety of plasma conditions (*i.e.* various RF power levels and exposure times) were then studied by XPS. As can be seen on the survey spectra given in Figure 8, oxygen plasma treatments (power density: 0.53 W.cm^{-2}) for 5 s and 30 min of exposure, respectively, are firstly responsible for a significant reduction of the amount of surface carbon. This results

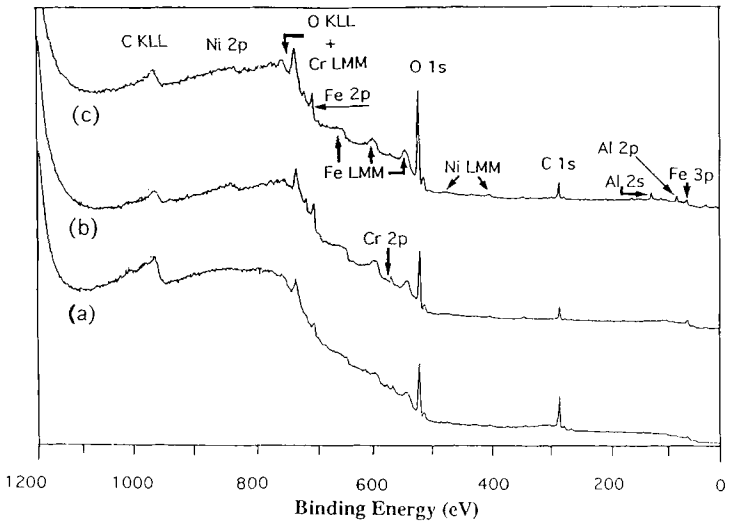

FIGURE 8 XPS wide scans of AISI 304 L samples: (a) untreated, (b) and (c) treated in an O_2 plasma for 5 s and 30 min, respectively.

from the fact that the major part of the hydrocarbon contamination is removed by oxidation reactions, the CO, CO_2 and H_2O volatile reaction products being pumped away in the vacuum system. As already shown in the case of an AISI 430 stainless steel[25] the main changes occurring concern the relative amounts of the alloying elements present in the oxidized surface layer. Indeed the O_2 plasma treatment produces a strong chemical erosion coupled with oxidation which particularly involves chromium. The effects of such a treatment (plasma exposure for 2, 5, 15, 30 s, 10 and 30 min, respectively) on the chromium surface content were followed by XPS, and the relevant spectra are presented in Figure 9. From the first seconds of treatment onwards noticeable changes occur in the Cr 2p photopeaks, originally characteristic of Cr in the CrO_3 form (Cr 2p 3/2 at 577.2 eV). For 2 s of O_2 plasma exposure onwards, a shoulder is already visible on the high binding energy side of the Cr 2p 3/2 and 2p 1/2 photopeaks. This shoulder increases with exposure time while the intial photopeak progressively decreases and practically disappears after 10 min of treatment. The new photopeak (Cr 2p 3/2 at 579.5 eV) characterizes a higher oxidation state of chromium which corresponds to the CrO_3 chemical form as indicated in the literature.[27] CrO_3 is the only form, according to its physical properties, that is susceptible of being vaporized under ion bombardment of the sample subjected to the plasma. This explains the disappearance of surface chromium from the stainless steel substrate during the O_2 plasma treatment. It should be noted that the kinetics of the disappearance of the surface chromium depend largely on the stainless steel composition and thermomechanical history of the corresponding sheets. For example, with similar experimental parameters, the AISI 304 L requires greater time of exposure to the O_2 plasma (*i.e.* more than about 30 min) than AISI 430 (*i.e.* about 5 min)[25] to attain the final state, *i.e.*

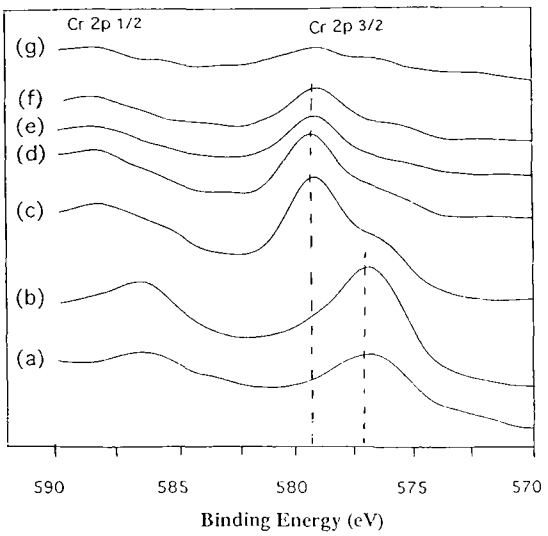

FIGURE 9 High resolution Cr 2p XPS spectra of AISI 304 L samples: (a) untreated, (b) to (g) treated in an O_2 plasma for 2, 5, 15, 30 s, 10 and 30 min, respectively.

disappearance of the surface chromium. Under these conditions, it must be expected that, as for AISI 430, the bond strength of adhesive/AISI 304 L systems varies largely with treatment duration given that, firstly, the presence and progressive disappearance of the Cr_2O_3 oxide and, furthermore, the presence and progressive disappearance of the CrO_3 oxide, play a key role in the adhesion properties of such systems.

Concerning again AISI 304 L stainless steels, Figure 10 represents Cr-Fe ISS spectra of samples which were (a) ultrasonically-cleaned in acetone for 7 min, (b) sandblasted according to an industrial procedure, (c) chemically-etched in a phosphoric acid bath, and (d) anodized in a concentrated nitric acid bath under galvanostatic conditions ($0.5\,mA\,cm^{-2}$, 1 h, room temperature, stainless steel cathode).[28] The spectra were obtained with Ne^+ ions in order to separate better the Cr and Fe components. They indicate that the chromium-to-iron ratio is greatest in the outer atomic layer of the anodized substrate. This result is interesting because the presence of chromium, in the oxide form, is known to promote adhesion properties of stainless steels.[28,29] In this context, Figure 11 shows how practical adhesion (three-point flexure test measurements) of rubber/primer/AISI 304 L systems change as a function of ageing time in humid atmosphere at 50°C. Clearly, the unaged assemblies have almost similar bond strengths but systems including anodized substrates have better performance than systems involving chemically-modified substrates.[30]

The next example relates to phosphate conversion layers built up on zinc-coated steels (hot-dipped galvanized steels) commonly used in the automotive industry. Such phosphate layers, deposited in the present work from a tri-cation (Zn^{2+}, Ni^{2+}, Mn^{2+}) phosphatizing solution (pH = 3, 55°C, 2 min), are used to improve the corrosion resistance of paint-steel systems. The investigation described here was undertaken by FTIR so as to characterize the behavior of such layers and, in particular, to determine how the amount of water contained in the corresponding phosphate crystals varies when samples are subjected to heating. This study was performed *in-situ*, using the heating cell in the reflection mode with an incidence angle of about 45°. A good

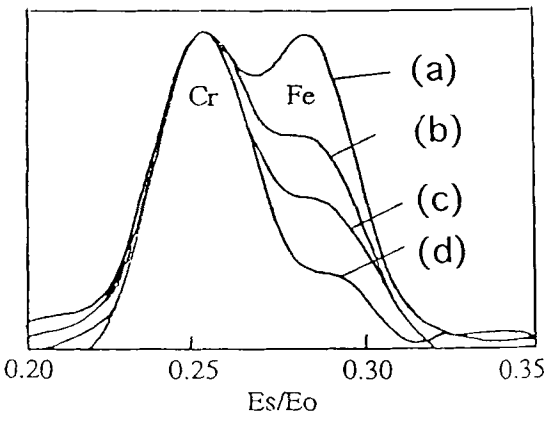

FIGURE 10 Chromium and iron ISS spectra (Ne^+ ions, 2 keV; scattering angle = 135°) of AISI 304 L samples: (a) untreated, (b) sandblasted, (c) etched in phosphoric acid and (d) anodized in nitric acid.

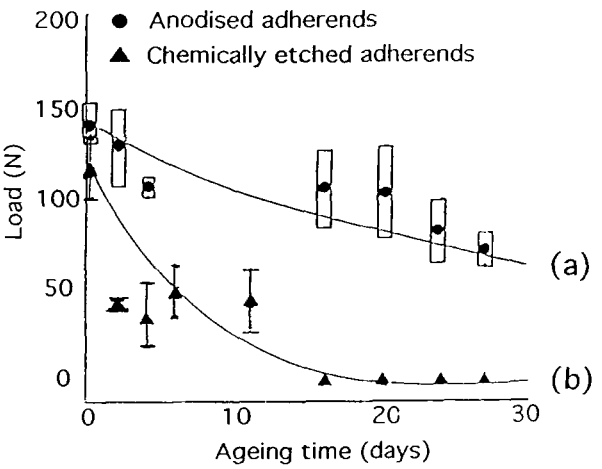

FIGURE 11 Bond strength evolution (three-point flexure test measurements) *vs.* ageing time of rubber/primer/AISI 304 L assemblies for (a) chemically-etched and (b) anodized substrates.

correlation is noted between the data provided by the two water absorption bands at about 3300 and 1640 cm^{-1} (Fig. 12). The water loss proceeds in two steps that could be roughly related to the loss of two molecules of water each in two stages as reported in the literature.[31,32] Such an experiment can be of great help to fit the paint or adhesive curing cycle to the properties of the conversion layer.

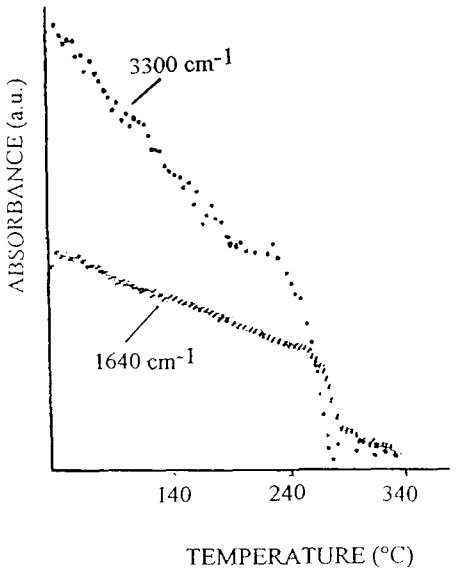

FIGURE 12 In-situ sudy in an FTIR heating cell of the water loss of phosphate layers on a zinc-coated steel.

Surface grafting

Another way of modifying metallic substrates consists of depositing very thin organic films a few molecular monolayers thick *via*, if possible, chemisorption mechanisms. In this context, we may cite the deposition of self-assembled monolayers (SAM).[33,34] By way of example, Figure 13 relates to experiments carried out in our laboratory concerning the chemisorption of n-alkyl thiol monolayers of different chain lengths on gold substrates. The shape of these plots, showing the evolution of the OSEE signal intensity against time, highlights the sensitivity of this technique with respect to the detection of such thin films. Applications of this technique to study surface functionalization (*e.g.* silanization) or certain adsorption phenomena is therefore possible, obviously by taking into account the aforementioned limitations concerning the capabilities of OSEE to distinguish different phenomena occurring simultaneously.

We may envisage the use of various low molecular weight coupling agents which are capable of forming chemical bonds across the polymer/metal interface. In a first step, we have studied the potential of organosulfurized derivatives, *viz.* n-alkyl thiols $SH\text{-}(CH_2)_n\text{-}CH_3$ with $n = 2, 5, 7, 11$ and 15, which are known to coordinate strongly to gold surfaces with the probable formation of thiolates RS-Au (I).[33] In these experiments, the surfaces were obtained by a sputtering process in order to deposit gold films about 60 nm in thickness on stainless steel or aluminum substrates, and ordered organic monolayers were adsorbed for 12 hours at room temperature from 10^{-3} M solutions of thiols in ethanol or heptane. The thiol-covered substrates were then rinsed in the corresponding solvent and blown dry with a stream of nitrogen. Spectroscopic characterization of the chemisorbed thiols was performed using LEEIXS. The increase of the CK_α emission band intensity is shown in Figure 14 as a function of the number of carbon atoms in the adsorbed thiols. The change in curve slope indicates a grafting density that is greater for long-chain thiols. The use of the three-point flexure test shows that failure occurs at the epoxy-coupling agent interface when long-chain thiols are

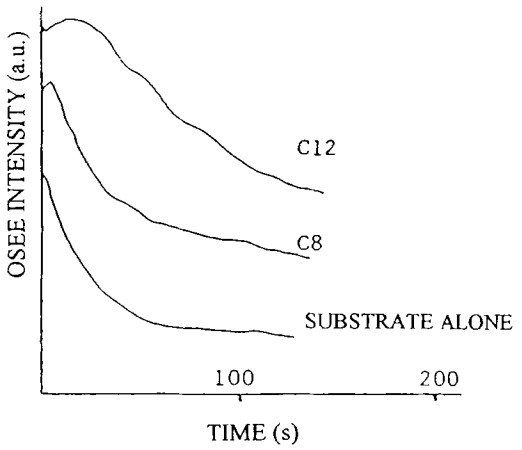

FIGURE 13 OSEE intensity evolution *vs.* time for a gold substrate covered with a self-assembled monolayer of alkyl thiols of different hydrocarbon chain lengths.

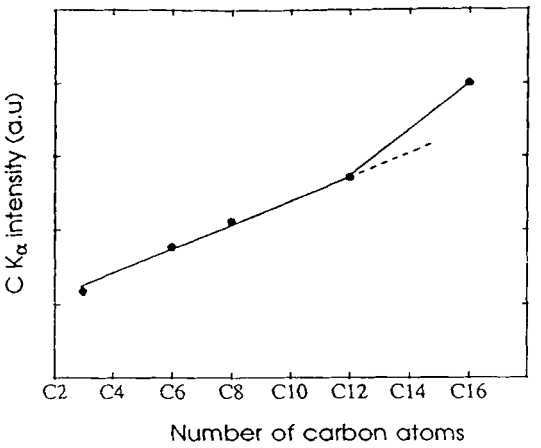

FIGURE 14 Absorption of n-alkyl thiols on gold substrates: variation of the C K_α intensity (LEEIXS measurements) *vs.* chain-length.

used (*e.g.* $n = 15$). This behavior can obviously be attributed to the fact that methyl groups are non polar and hydrophobic but also to the fact that thiols form a densely-packed, crystal-like assembly as chain length increases. On the contrary, failure takes place at the stainless steel-gold or aluminum-gold interfaces when short-chain thiols are used (*e.g.* $n < 7$). This behavior can be explained by the fact that, as chain length decreases, the monolayer assembly structure becomes increasingly disordered with lower packing density and coverage which leads to easier access of the adhesive within the chains of the coupling agents towards the metallic substrate. Under these conditions, it is clear that the bonded specimen part which is less resistant when a mechanical test is carried out, is no longer that which is located at the interface between the coupling agent and the epoxy as in the previous case, but rather that located at the interface between the gold film and the metallic substrate, whatever the latter may be (stainless steel or aluminum). Studies are in progress in such fields using mercaptoesters or other bifunctional molecules which can react chemically with the epoxy functions of the resins.

Surface Characterization of Failed Specimens

In adhesive bonding, detailed failure analysis, including both identification of the actual locus of failure and understanding of the reason why a manufactured product or a test structure has debonded, is obviously of prime importance for improving the performances of the corresponding complex systems. Indeed, such an analysis must, in principle, allow one to identify the weakest link of the bonded joint and, therefore, to propose a strengthening solution of the zone concerned *via*, for instance, the change of the adherend-pretreatment procedure, the use of a suitable coupling agent, the replacement of the adhesive or the fabrication process.

In this context, Figure 15 relates to a polyester-steel industrial system. In this work, a failed peel test specimen was investigated by micro-FTIR under grazing incidence

FIGURE 15 Analysis by micro-FTIR under grazing incidence (GAMFTIR) of the metal side of a polyester-steel assembly after failure under a peel test.

(GAMFTIR).[35,36] The analyzed area was about 100 μm in diameter and the analysis was performed at random over the delamination propagation zone. Some characteristic spectra gathered in Figure 15 indicate a very thin layer of polymer remaining at the sample surface after failure occurs. This is shown clearly by the $\nu(C=O)$ infra-red absorption band at about 1720 cm^{-1}. The thickness of the remaining polymer layer can be estimated to be about 20 nm. These experiments show that it is of vital interest to use GAMFTIR to highlight such cohesive failures, since less-sensitive conventional micro-FTIR (at near normal incidence) would erroneously indicate an interfacial-like failure.

The last example deals with an epoxy-aluminum joint. It must be recalled that surface chemical properties of the corresponding substrate largely govern the adhesive-adherend interactions and the long-term resistance of the joint to adverse environmental effects and that suitable surface treatments, essentially via chemical or electrochemical processes, have been developed to provide stronger and more durable systems. However, it should also be noted that improvement of joint performance is often associated with changes in the locus of the failure when mechanical tests are used, and that it is necessary to characterize areas of some tens of μm in diameter at the failed sample surface. In the present work, aluminum samples, subjected either to (a) mere degreasing (stabilized 1, 1, 1-trichloroethane) or to (b) degreasing followed by a sulfuric-chromic acid etching (optimized FPL-type process) at 60°C for 25 min, were bonded with an epoxy adhesive and relevant bonded joints were subjected to the three-point flexure test. After failure under test, the delamination initiation zone (less than 100 μm in diameter) was investigated by micro-FTIR in the reflection mode. As largely reported in the litera-

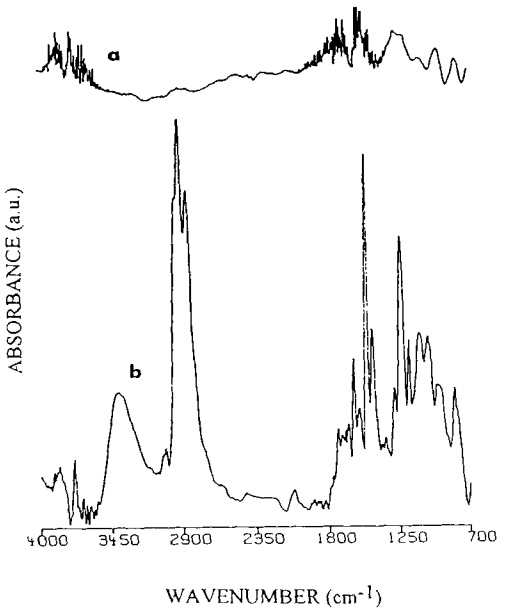

FIGURE 16 Analysis by micro-FTIR of the failure initiation zone (about 100 μm in diam) in epoxy-aluminum three-point flexure test specimens. Aluminum was subjected to (a) degreasing or (b) sulfuric-chromic acid etching.

ture,[22,23,37,38] the etching treatment improves the adhesion performance, but also often modifies the failure locus as indicated by the spectra in Figure 16. After such a chemical surface treatment, the failure clearly occurs within the polymer and indicates that a suitable solution has been found to this specific adhesion problem.

CONCLUSION

The few examples described in this paper show that many surface and near-surface analytical and characterization techniques allow a better understanding of (i) the changes in chemistry of adherends due to surface treatments and, therefore, of the sources of contamination which could affect adhesive bonding and bonded joint properties, and (ii) where (and sometimes why) an adhesive joint fails during testing or service.

Obviously, all the techniques used in this work possess specific and generally well-known advantages and disadvantages but it is clear that missing information can always be obtained by using a variety of other methods not cited here even if difficulty in studying interfacial bonds remains.

References

1. J. S. Solomon, W. L. Baun, in *Surface Contamination Genesis, Detection and Control*, K. L. Mittal, Ed. (Plenum Press, New York, 1979), pp. 609–634.

2. W. L. Baun, in *Industrial Applications of Surface Analysis*, L. A. Casper, Ed. (American Chemical Society, Washington, 1982), ACS Symposium Series # 199, pp. 121.
3. W. L. Baun, in *Adhesion Aspects of Polymeric Coatings*, K. L. Mittal, Ed. (Plenum Press, New-York, 1983), pp. 131–146.
4. J. M. Walls, A. B. Christie, in *Surface Analysis and Pretreatment of Plastics and Metals*, D. M. Brewis, Ed. (Applied Science Publishers, London, 1982), pp. 13–44.
5. W. L. Baun, in *Surface Analysis and Pretreatment of Plastics and Metals*, D. M. Brewis, Ed. (Applied Science Publishers, London, 1982), pp. 45–72.
6. D. Briggs, in *Surface Analysis and Pretreatment of Plastics and Metals*, D. M. Brewis, Ed. (Applied Science Publishers, London, 1982), pp. 73–94.
7. J. P. Wightman, *Sampe Q.* **13,** 1–8 (1981).
8. G. D. Davis, J. D. Venables, in *Durability of Structural Adhesives*, A. J. Kinloch, Ed. (Applied Science Publishers, London, 1983), pp. 43–84.
9. W. J. Van Ooij, in *Industrial Adhesion Problems*, D. M. Brewis and D. Briggs, Eds. (Orbital Press, Oxford, 1985), pp. 87–127.
10. J. A. Filbey and J. P. Wightman, in *Adhesive Bonding*, L. H. Lee, Ed. (Plenum Press, New York, 1991), pp. 175–202.
11. M. Romand, R. Bador, M. Charbonnier, F. Gaillard, *X-Ray Spectrometry* **16,** 7–16 (1987).
12. M. Romand, F. Gaillard, M. Charbonnier, D. S. Urch, *Adv. in X-ray Analysis* **34,** 105–121 (1991).
13. M. Romand, F. Gaillard, M. Charbonnier, *Adv. in X-Ray Analysis* **35 B,** 767–781 (1992).
14. T. Smith, *J. Appl. Phys.* **46,** 4, 1553 (1975).
15. V. Rossiter, *Research and Development* **2,** 94 (1988).
16. A. Roche, M. J. Romand, F. Sidoroff, in *Adhesive Joints-Formation, Characteristics and Testing*, K. L. Mittal, Ed. (Plenum Press, New York, 1984), p. 19–30.
17. A. Roche, F. Gaillard, M. Romand, M. von Fahnestock, *J. Adhesion Sci. Technol.* **1,** 2, 145–157 (1987).
18. M. Romand, *J. Adhesion* **37,** 109–120 (1992).
19. J. M. Sykes, in Surface Analysis and Pretreatments of Plastics and Metals, D. M. Brewis Ed. (Applied Science Publishers, London 1982), pp. 153–174.
20. A. C. Moloney, in Surface Analysis and Pretreatment of Plastics and Metals, D. M. Brewis Ed. (Applied Science Publishers, London 1982), pp. 175–197.
21. A. J. Kinloch, in *Adhesion and Adhesives: Science and Technology*, (Chapman and Hall, London, 1987), pp. 101–170.
22. H. M. Clearfield, D. K. Mc Namara, G. D. Davis, in *Adhesive Bonding*, L. H. Lee, Ed. (Plenum Press, New-York, 1991), pp. 203–237.
23. J. D. Minford, in *Adhesive Bonding*, L. H. Lee, Ed. (Plenum Press, New-York, 1991), pp. 239–290.
24. H. Kollek, W. Brockmann, in *Surface Contamination: Its Genesis, Detection and Control*, K. L. Mittal, Ed. (Plenum Press, New York 1979), pp. 713–721.
25. L. Deshayes, M. Charbonnier, N. S. Prakash, F. Gaillard, M. Romand, *Surf. Interface Anal.* **21,** 711–717 (1994).
26. L. Deshayes, Thesis, Univ. Claude Bernard, Lyon, 1993.
27. S. Storp, R. Holm, *Surf. Sci.* **68,** 10 (1977).
28. F. Gaillard, M. Romand, H. Hocquaux, J. S. Solomon, *Surf. Interface Anal.* **10,** 163 (1987).
29. R. P. Haak, T. Smith, *Int. J. Adhes. Adhes.* **1,** 5 (1983).
30. N. S. Prakash, A. Roche, M. Charbonnier, M. Romand, S. Portay, F. Alarcon-Lorca, in *Natural Rubber. Current Developments in Product Manufacture and Application*, A. Kadir, Ed. (Rubber Research Institute of Malaysia, Kuala Lumpur, 1993), pp. 347–357.
31. Y. Arnaud, E. Sahakian, M. Romand, *Appl. Surf. Sci.* **32,** 281–195 (1988).
32. E. Sahakian, Thesis, Univ. Claude Bernard, Lyon, 1989.
33. M. D. Porter, T. B. Bright, D. L. Allara, C. E. D. Chidsey, *J. Am. Chem. Soc.* **109,** 3559 (1987).
34. D. L. Allara, R. G. Nuzzo, *Langmuir* **1,** 45 (1985).
35. M. Sweeney, F. Gaillard, I. Linossier, N. Boyer, I. Stevenson, *Spectra 2000, Spectra Analyse* **176,** 33–38 (1994).
36. F. Gaillard, D. Verchere, H. Hocquaux, M. Romand, *J. Adhesion* **46,** 403–408 (1994).
37. G. D. Davis, in *Adhesive Bonding*, L. H. Lee, Ed. (Plenum Press, New-York, 1991), pp. 139–173.
38. M. Romand, M. Charbonnier, *Le Vide, les Couches Minces* **47,** 256, 127–173 (1991).